Ultramicroscopy 108 (2008) 1495–1499

Contents lists available at ScienceDirect

Ultramicroscopy

journal homepage: www.elsevier.com/locate/ultramic

Analysis of InAsN quantum dots by transmission electron microscopy and photoluminescence

Chiung-Chih Hsu [a,e,*], Ray-Quen Hsu [a], Yue-Han Wu [b], Tung-Wei Chi [c], Chen-Hao Chiang [d], Jenn-Fang Chen [d], Mao-Nan Chang [e]

[a] Department of Mechanical Engineering, National Chiao-Tung University, Hsinchu 30056, Taiwan, ROC
[b] Department of Materials Science and Engineering, National Chiao-Tung University, Hsinchu 30043, Taiwan, ROC
[c] Industrial Technology Research Institute, Hsinchu, Taiwan, ROC
[d] Department of Electrophysics, National Chiao-Tung University, Hsinchu, Taiwan, ROC
[e] Department of Nano Metrology, National Nano Device Laboratories, Hsinchu 30078, Taiwan, ROC

ARTICLE INFO

PACS:
68.65.+g
78.20
73.61.Ey

Keywords:
Quantum dots
TEM
PL
Molecular beam epitaxy

ABSTRACT

Quantum dots (QDs) have great potential in optical fiber communication applications were widely recognized. The structure of molecular beam epitaxy (MBE) grew InAsN QDs were investigated by transmission electron microscopy (TEM) and measured their optical properties by photoluminescence (PL). TEM images show that the InAsN QDs are irregular or oval shaped. Some of the InAsN QDs are observed to have defects, such as dislocations at or near the surface in contrast to InAs QDs, which appear to be defect free. PL results for InAsN QDs showed a red-shifted emission peak. In addition, the InAsN emission peak is broader than InAs QDs, which supports the TEM observation that the size distribution of the InAsN QDs is more random than InAs QDs. The results show that the addition of nitrogen to InAs QDs leads to a decrease in the average size of the QDs, bring changes in the QD's shape, compositional distribution, and optical properties.

© 2008 Published by Elsevier B.V.

1. Introduction

Quantum dots (QDs) have been observed in many materials systems, i.e., In(Ga)As/GaAs [1,2], InP/InGaP [3], GaSb/GaAs [4],and InAs/InP [5,6]. The self-assembled Stranski–Krastanow--mode QDs, have many desirable properties that could be useful in communication applications. These kinds of QDs have a low threshold current, high saturation material gain, and differential gain. At present, InP substrates quantum dots were used in optical fiber communication industry. However, the costs of these materials and their fragility have limited their widespread adoption. By using GaAs substrates in place of InP substrates, the cost will be significantly decreased and will also potentially produce a yield of higher-quality quantum dots with longer emission wavelengths. In recent years, many researchers have studied InAs QDs on GaAs and have found that it is difficult to push the emission maxima to the desirable 1.5 μm. Another big drawback for InAs QDs is the large lattice mismatch between InAs and GaAs. The lattice mismatch can be reduced by introducing nitrogen into InAs QDs [7,8] and a lower band gap can be obtained [9–11]. Many investigators believe that the laser emission wavelength can reach 1.3 or 1.55 μm due to the fact that the smaller lattice mismatch between the quantum dots and host material will reduce strain and therefore reduce defects during fabrication [8]. Follow the previous theory, nitrogen will diffuse into InAs QDs resulting in a lower band gap. This could be expected to extend their emission wavelength. However, the addition of nitrogen into InAs QDs often induces defects. These defects lead to a decreased intensity of the PL emission peak. The mechanism of this phenomenon is still unknown. The purpose of this investigation is to study the influence of the presence of nitrogen in InAsN QDs, their optical properties, compositional distribution, and shape.

2. Experiments

InAsN QDs were grown by molecular beam epitaxy (MBE) on (0 0 1) n-type GaAs substrates with a nitrogen source radio-frequency plasma as shown in Fig. 1. In order to decrease the lattice mismatch between InAs and the GaAs substrate, nitrogen was added to form InAsN QDs. At first, a GaAs buffer layer with a thickness of 0.3 μm was grown on a substrate at 600 °C. Next, InAs(N) QDs were grown with a nitrogen source radio-frequency plasma at a lower growth rate and a growth temperature between

* Corresponding author at: Department of Mechanical Engineering, National Chiao-Tung University, Hsinchu 30056, Taiwan, ROC.
E-mail address: sctndl@gmail.com (C.-C. Hsu).

0304-3991/$ - see front matter © 2008 Published by Elsevier B.V.
doi:10.1016/j.ultramic.2008.04.098

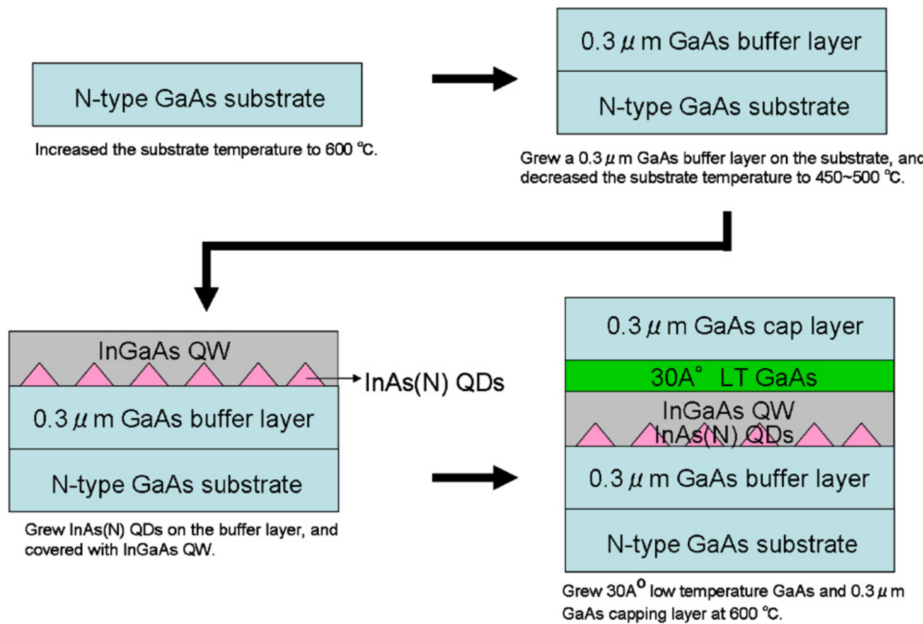

Fig. 1. The flow chart of sample structure.

485 and 500 °C. (<1.86 Å/s). During the growth of the InAsN QDs, we introduced 17% atomic percent of nitrogen into the growth conditions. InAs quantum dots were grown without nitrogen present. The InGaAs quantum well was grown to a thickness of 50 Å at the same temperature. Finally, a capping layer was grown under the same conditions as the GaAs buffer layer. The emission wavelength of the quantum dots were characterized by PL. The PL of the InAsN QDs was obtained by a power density of 130 mW. On the other hand, the PL of the InAs QDs used a power density of 1.3 mW. The PL experiments were preformed at 300 K.

The samples were polished by sandpaper and diamond paper and then pruned and cleaned by an Ar+ ion miller with an accelerating voltage of 5 keV, rotation speed of 3.5 rpm, and an incident angle of 5°. Evaluation of InAs QDs and InAsN QDs' morphology and structure were conducted with TEM, JEOL-2010F, along the (1 0 0) and (1 1 0) orientations. Compositional distributions were characterized by scanning transmission electron microscopy (STEM, EM24015), and energy dispersive spectrometer (EDS, INCA IET250).

3. Results and discussion

Fig. 2(a) and (b) show the quantum dots in high-angle annular dark field (HAADF) STEM images taken from two samples. We also measured the dimension of the QDs from HAADF STEM images. The height is defined as the distance measured from the top of quantum dots to the interface of InGaAs quantum well (QW) and GaAs substrate; the diameter of the QDs is the dimension measured from right side to left side of quantum dots bottom as shown in Fig. 3. The average size of the InAs QDs was 27.0 nm in diameter and 10.9 nm in height. The average size of InAsN QDs was 17.4 nm in diameter and 10.0 nm in height. InAsN QDs were somewhat smaller, however, the QDs density decreased compared to InAs QDs sample. The estimated densities of the quantum dots for the two different samples were $1.02 \times 10^{10}\,cm^{-2}$ for InAs QDs and $0.5 \times 10^{10}\,cm^{-2}$ for the InAsN QDs. Their size distributions are shown in Fig. 3(a) and (b). The InAs QDs were more uniform in size and their shapes were more oval. On the contrary, the InAsN QDs size distribution was more random. Large QDs and small QDs co-existed in the InAsN QDs sample. Some of the InAsN QDs size and shape were similar to the InAs QDs, but most of the InAsN QDs size and shape were different. This phenomenon may result from the incorporation of nitrogen into the quantum dots. In order to observed the structure in detail, fast Fourier filtered images of InAsN QDs and EDS experiments focusing on Indium were performed. Because the samples were made by MBE under high-vacuum conditions, the samples are not expected to contain oxides. The original high-resolution TEM image of QDs showed lattice fringes in exact (1 0 0) zone axis. So, using fast Fourier filtered images from the high-resolution TEM images, a deeper insight was obtained of the structural detail of InAs QDs and InAsN QDs. The 'Moiré fringes' pattern was observed. The Moiré fringes originated from the InAs QDs and InAsN QDs. For the InAs QDs' Moiré fringes showed negligible defects in the quantum dots (see Fig. 4(a) and (b)). In contrast, the InAsN QDs' Moiré fringes showed dislocations clearly visible along the surface of InAnN QDs (see Fig. 4(c) and (d)). This observation may explained by the reduction of boundary strain energy while the nitrogen atoms were incorporated. This implies that the InAsN QDs were plastically relaxed as well, an observation that is consistent with quantum dots grown from curved surfaces [12]. It was assumed that nitrogen could be incorporated from the (0 0 1) facet and that it accumulates at the surface, thus stimulating dislocations and changing the surface energy. Images of 10 sets of top and bottom points were taken for both the InAs and InAsN QDs for quantitative analysis. It was further observed that the indium concentration fluctuated within individual QDs. The indium migrates away from the surface and into the InAsN QDs because of the presence of nitrogen (in Table 1). Also, the indium content distribution tended to be below that of InAsN QDs, and even the wetting layer. This reveals that a wetting layer beneath the InAsN QDs was formed (see Fig. 2(b)). Its thickness was approximately 2.6 nm. The increased nitrogen supply was related to indium migration in the quantum dots. This activity affected the formation and size of the InAsN QDs. As a result of nitrogen incorporation, the indium stayed away from the InAsN QDs and the averaged size of the QDs decreased.

It has been reported that the PL spectrum of these QDs is affected by nitrogen being added into the quantum dots and this

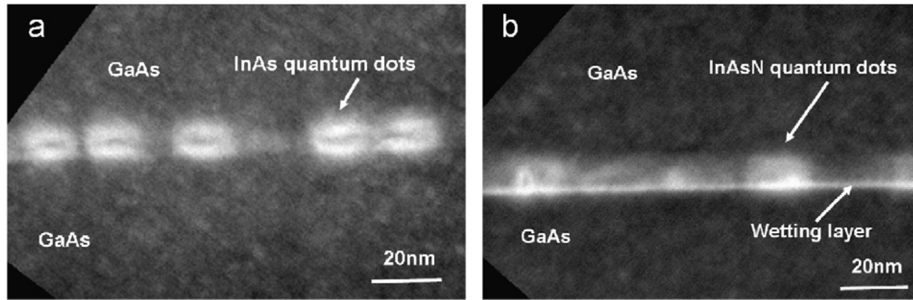

Fig. 2. Cross-sectional HAADF STEM images of (a) InAs QDs sample (b) InAsN QDs sample.

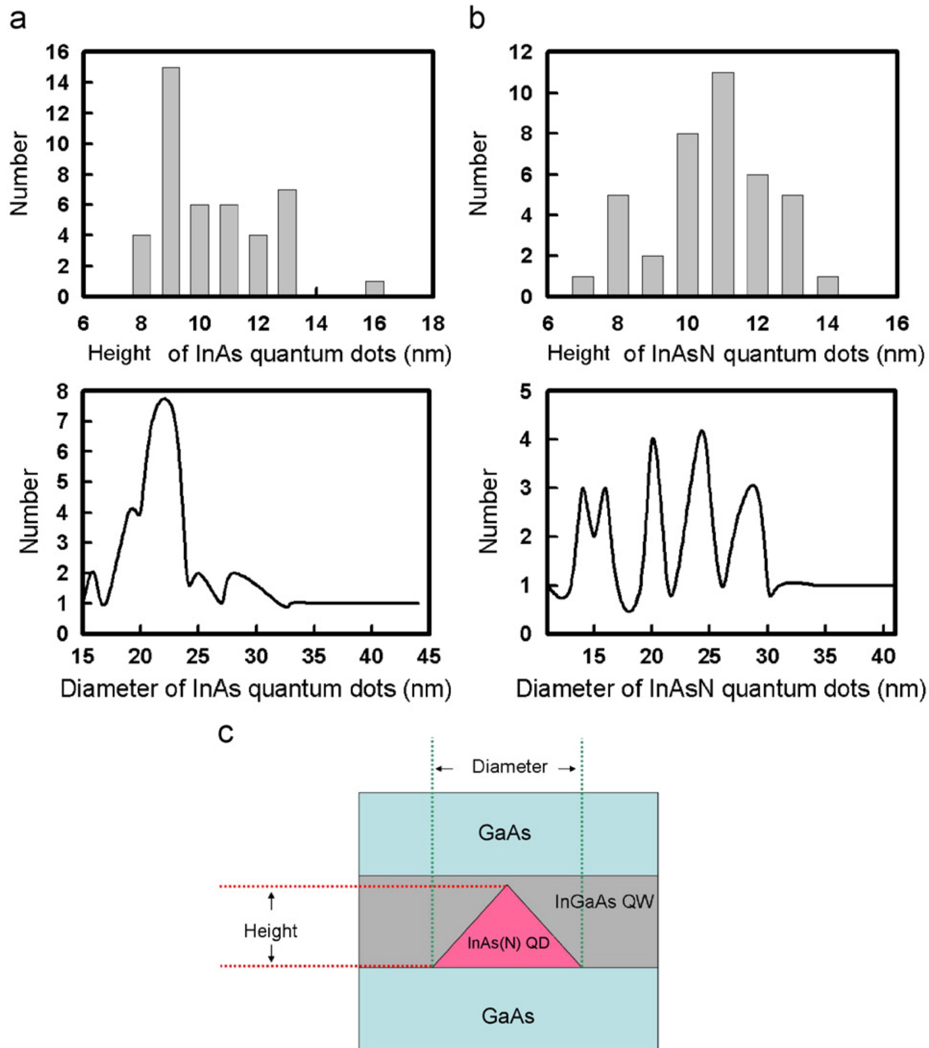

Fig. 3. Distributions of diameter size and height size in InAs QDs and InAsN QDs: (a) InAs QDs, (b) InAsN QDs, and (c) measure model.

leads to a decrease of the band gap and confinement [13]. A different laser power of 1.3 and 130 mW at a temperature of 300 K was applied to the InAs QDs and InAsN QDs, respectively, the emission wavelength of two peaks were 1200 and 1310 nm for InAs QDs. In contrast, the emission wavelength of the InAsN QDs shifted slightly and had peaks of 1250 and 1350 nm as shown in Fig. 5. The results show two peaks in PL allowing us to find the band gaps of ground and first excited states simultaneously. The addition of nitrogen lead to a decrease in the band gap, however, it did not change drastically. This result could also be explained by the dislocations that were located in the InAsN QDs. If the charge carriers were trapped, as a result of the dislocations, the red-shift phenomenon would be eliminated. The PL intensity dropped drastically because of the presence of dislocations in the InAsN QDs. It was found that the first peak of InAsN QDs was similar to InAs QDs, therefore its emission value was nearly the same as the InAs QDs. The second peak of InAsN QDs was observed from the other random quantum dots. It was also found that InAs QDs's PL peaks full-width at half-maximum (FWHM) was narrow and the quantum dots were uniform in size. On the other hand, regardless

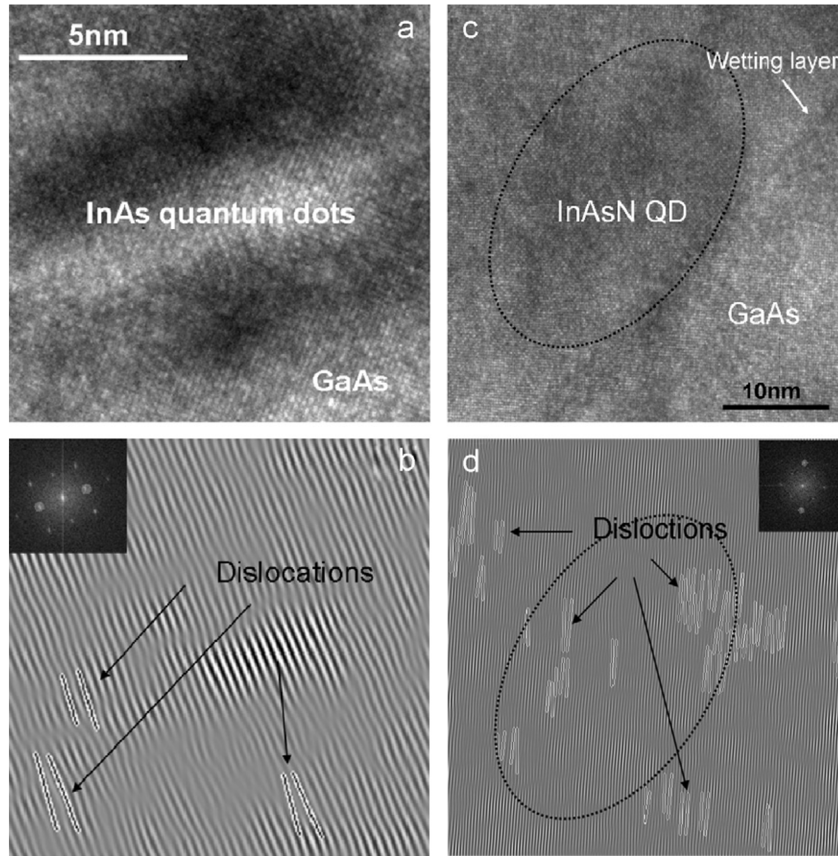

Fig. 4. InAs quantum dots observed along the (1 0 0) orientation. (a) HR TEM image. (b) Fast Fourier filtered image. InAsN quantum dots observed along the (1 0 0) orientation. (c) HR TEM image. (d) Fast Fourier filtered image.

Table 1
Indium distributions in the quantum dots

		Element	Weight%	Atomic%
(a) InAs quantum dots				
	★1	Ga K	39.89	43.31
		As L	48.59	49.09
		In L	11.52	7.59
	★2	Ga K	39.67	42.55
		As L	52.35	52.25
		In L	7.98	5.20
(b) InAsN quzntum dots				
	★1	Ga K	50.77	52.71
		As L	48.44	46.80
		In L	0.79	0.50
	★2	Ga K	48.33	51.24
		As L	45.20	44.59
		In L	6.47	4.17

of the first or second peak of InAsN QDs, the FWHM was broader than that of the InAs QDs. These peaks of InAsN QDs were broad due to the random quantum dot sizes. Another observation was that both InAs QDs and InAsN QDs had two peaks in the PL spectra. This implies that there were bimodal size distributions among both samples. This result was confirmed by HAADF STEM images.

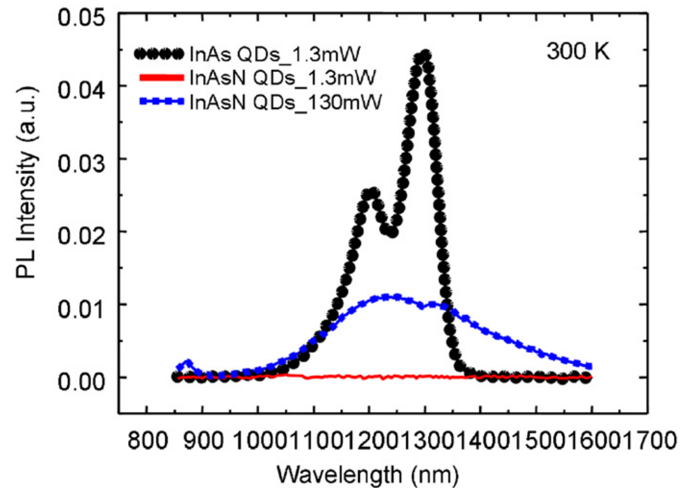

Fig. 5. The PL of InAsN QDs and InAs QDs at 300 K.

4. Conclusion

The average size of InAsN QDs was smaller than the InAs QDs. The high-resolution images of InAsN QDs taken with fast Fourier transform processing, HAADF STEM images and EDS experiments

of Indium showed that nitrogen did incorporate into the quantum dots. The indium was found migrate below the quantum dots into the wetting layer. It was observed, the InAsN QDs shapes were irregular or oval shaped. The InAs QDs shapes were mostly oval shaped. From PL analysis, InAsN QDs red-shift slightly due to the nitrogen caused dislocations.

Acknowledgments

The authors are grateful to Dr. Steven Kooi at Institute for Soldier Nanotechnologies Massachusetts Institute of Technology for his advice.

References

[1] J.M. Gerald, J.B. Genin, J. Lefebvre, J.M. Moison, N. Lebauche, F. Barthe, J. Cryst. Growth 150 (1995) 351.
[2] D. Leonard, K. Pond, P.M. Petroff, Phys. Rev. B 50 (1994) 11687.
[3] A. Kurtenbach, K. Eberl, T. Shitara, Appl. Phys. Lett 66 (1995) 361.
[4] F. Hatami, N.N. Ledentsov, M. Grundmann, J. Bohrer, F. Heinrichsdorff, M. Beer, D. Bimberg, S.S. Ruvimov, P. Werner, U.G. osele, J. Heydenreich, U. Richter, S.V. Ivanov, B.Y. Meltser, P.S. Kop'eV, Z. Alferov, Appl. Phys. Lett 67 (1995) 656.
[5] V.M. Ustinov, E.R. Weber, S. Ruvimov, Z. Liliental-Weber, A.E. Zhukov, A.Yu. Egorov, A.R. Kovsh, A.F. Tsatsul'nikov, P.S. Kop'ev, Appl. Phys. Lett 72 (1998) 362.
[6] Sun Zhongzhe, Soon Fatt Yoon, Yew Kuok Chuin, J. Cryst. Growth 259 (2003) 40.
[7] M. Kondow, K. Uomi, A. Niwa, T. Kitatani, S. Watahiki, Y. Yazawa, Jpn. J. Appl. Phys. Part 1 35 (1996) 1273.
[8] O. Schumann, L. Geelhaar, H. Riechert, H. Cerva, G. Abstreiter, J. Appl. Phys. 96 (5) (2004) 2832.
[9] I.A. Buyanova, W.M. Chen, B. Monemar, MRS Internet J. Nitride Semicond. Res. 6 (2001) 2.
[10] M. Kuroda, A. Nishikawa, R. Katayama, K. Onabe, J. Cryst. Growth 278 (2005) 254.
[11] H. Tsurusawa, A. Nishikawa, R. Katayama, K. Onabe, Phys. Stat. Solidi (b) 243 (7) (2006) 1657.
[12] A. Ueta, K. Akahane, S. Gozu, N. Yamamoto, N. Ohtani, Phys. Stat. Solidi (b) 243 (7) (2006) 1514.
[13] V. Sallet, G. Patriarche, M.N. Merat-Combes, L. Largeau, O. Mauguin, L. Travers, J. Cryst. Growth 290 (2006) 80.